Endoscopic Image Classification using Edge-Based Features

M. Häfner [1], A. Gangl [2], M. Liedlgruber [3,*], A. Uhl [3], A. Vécsei [4], and F. Wrba [5]

[1] Department for Internal Medicine, St. Elisabeth Hospital, Vienna
[2] Department of Gastroenterology and Hepatology, Medical University of Vienna, Austria
[3] Salzburg University, Department of Computer Sciences, Austria
[4] St. Anna Children's Hospital, Vienna, Austria
[5] Department of Clinical Pathology, Medical University of Vienna, Austria
[*] *Corresponding author e-mail: mliedl@cosy.sbg.ac.at*

Abstract

We present a system for an automated colon cancer detection based on the pit pattern classification. In contrast to previous work we exploit the visual nature of the underlying classification scheme by extracting features based on detected edges. To focus on the most discriminative subset of features we use a greedy forward feature subset selection. The classification is then carried out using the k-nearest neighbors (k-NN) classifier.

The results obtained are very promising and show that an automated classification of the given imagery is feasible by using the proposed method.

1 Introduction

Today the gold standard for colon examination is colonoscopy which is performed by using a colonoscope. Modern colonoscopes are able to take pictures from inside the colon which allows to obtain images for a computer-assisted analysis with the goal of detecting tumorous lesions. To get highly detailed images a magnifying endoscope is used [1], which represents a major advance as it provides images which are up to 150-fold magnified, thus uncovering the fine surface structure of the mucosa as well as small lesions.

In this work we present an automated classification system aiming at colon cancer detection. While in previous work we mainly focused on general-purpose texture features, we now aim at exploiting the visual nature of the cancer classification scheme used.

This work is partially funded by the Austrian Science Fund (FWF) under Project No. L366-N15 and by the Austrian National Bank "Jubiläumsfonds" Project No. 12514

In Section 2 we review the classification of pit patterns of the colonic mucosa. Section 3 describes the feature extraction process and the classification used in our proposed method. Experimental results and configuration details of our system are given in Section 4. Section 5 concludes the paper.

2 Pit Pattern Classification

Polyps of the colon are a frequent finding and are usually divided into metaplastic, adenomatous, and malignant. As resection of all polyps is time-consuming, it is imperative that those polyps which warrant endoscopic resection can be distinguished: polypectomy of metaplastic lesions is unnecessary and removal of invasive cancer may be hazardous. For these reasons, assessing the malignant potential of lesions at the time of colonoscopy is important.

The pit pattern classification, originally reported by Kudo et al. [6], is the most commonly used classification system to distinguish between non-neoplastic and neoplastic lesions in the colon. It differentiates between six different types according to the mucosal surface of the colon, as shown in Figure 3 (type 3 is divided into 3S and 3L designating the size of the pit structure). This classification system allows to assess the malignant potential of a lesion based on the visual pattern of the mucosal surface. Thus, it is a convenient tool to decide which lesions need not, which should, and which most likely can not be removed endoscopically.

Lesions of type 1 and 2 can be grouped into non-neoplastic lesions and types 3 to 5 can be grouped into neoplastic lesions, where type 5 is highly indicative for cancer. This allows a grouping into two classes, which is more relevant in clinical practice [5].

Using a magnifying colonoscope together with indigo carmine dye spraying, the mucosal crypt pattern on the surface of colonic lesions can be observed [7]. Several studies found a good correlation between the mucosal pit pattern and the histological findings, where especially techniques using magnifying colonoscopes led to excellent results [5]. Due to the visual nature of this classification scheme it is also a convenient choice for an automated image classification.

3 Proposed Approach

In the past we have shown that an automated classification of magnified endoscopic images based on the pit pattern scheme is feasible. But in our previous work we mainly focused on general purpose features describing texture properties (e.g. [4, 3]).

By contrast, the proposed method is based on the visual structures of the pits, using segmentation into pit areas and background and two types of features (shape and texture). Besides that, unlike the approaches presented in [4, 3], this method is not dependent on a time-consuming transformation to extract features.

3.1 Feature Extraction and Classification

Pre-processing: Prior to the edge detection we downscale the image by a half to obtain a low-resolution image and reduce artifacts. Then we apply anisotropic diffusion to each color channel of the source image to suppress noise and preserve edges at the same time [8]. While anisotropic diffusion could also be applied to all color channels at once, we separately pre-process each color channel since the edges are extracted from separate color channels too. Furthermore we use Contrast Limited Adaptive Histogram Equalization (CLAHE) [9] to fix inhomogeneous brightness and contrast.

Binarization: Afterwards, we perform a global thresholding to obtain a binary image. This binary image is then upsampled to the original image size.

Morphological pre-processing: Then we pre-process the binary image by using a set of morphological operators. First we apply a closing to remove small "holes", using a disk of radius 1 as structuring element. This radius has been chosen to not disturb the shape of the pits too much but to only fill small holes and remove small notches eventually present along the borders of pit areas. Then we bridge unconnected pixels by setting pixels to white which lie between two unconnected, white neighbors (using a 3×3-neighborhood). Furthermore we remove isolated pixels followed by filling closed regions. Finally, we set pixels to black which have less than five white neighbors (if only half of the pixels in the 3×3-neighborhood or less are white). This step helps to minimize the number of small spurs which might eventually have endured the previous steps.

ID	Short description
F1	mean of average intensity within each pit
F2	number of pits found
F3	mean of average energy (sum of squared intensities) within each pit
F4	mean area over all pits
F5	fraction of polygons having a perimeter above the median of all perimeters
F6	mean dispersion (max radius from the pit center to the pit boundary divided by the pit area) over all pits
F7	mean of average saturation within each pit (HSV)
F8	mean of average hue within each pit (HSV)
F9	mean triangle area computed from a delaunay triangulation based on the pit centers
F10	mean edge length computed from a delaunay triangulation based on the pit centers
F11	mean compactness (area divided by the squared perimeter) over all pits
F12	mean perimeter of pits found
F13	sum of average intensity within each pit
F14	sum of average hue within each pit (HSV)
F15	sum of average saturation within each pit (HSV)
F16	intensity mean of the pre-processed channel (after applying anisotropic diffusion and CLAHE)
F17	intensity mean of the original channel
F18	mean irregularity (max radius from the pit center to the pit boundary divided by the minimum radius from the pit center to the pit boundary) over all pits

Table 1. Chosen set of possible features.

Edge detection: Performing edge detection on the color channels often results in too many edges or quite a few polygons which are not closed. Hence, we extract the edges from the binary image resulting from the morphological pre-processing. To extract edges we use the Canny edge detector ($\sigma = 1.5$) without multi-resolution feature synthesis [2] which may produce polygons which are not closed.

Morphological post-processing: Thus we post-process the edges by using the morphological operators from above, except for the closing (in the same order). Then we again remove isolated pixels and interior pixels of the white areas to obtain the final edge map.

This processing of the binary map and edges ensures that we end up with closed polygons only, which are smooth and free of unwanted artifacts. This is because of the filling of closed areas (which does not affect polygons which are not closed as can be seen in Fig. 1(e)) and subsequently removing white pixels, which do not belong to borders of filled areas (see Fig. 1(f)). Apart from that we see from Fig. 1(a) that some images contain ridges which can be considered to be artifacts. These are removed by the post-processing. An undesired side-effect of this post-processing is that pits touching the border are removed too.

Finally, we trace all edges to obtain the location of the border pixels for each detected polygon. Some of these steps are illustrated in Fig. 1(a)-(g).

Feature selection: We consider features which are based on the shape of the pit areas and features which are based on the pixel intensities within the pit areas (see Table 1). Fig. 3 shows examples of detected pit areas for each pit type. Since the optimal set of features is not known we construct a feature candidate set consisting of all possible features from all color channels considered. Then we use a greedy forward selection algorithm to find the feature subset yielding the best total

(a) (b) (c) (d) (e) (f) (g)

Figure 1. Edge detection steps (a) red channel of an input image, (b) pre-processing, (c) thresholding, (d) Canny edge detection, (e) the pits (filled white) and the parts to be discarded by the edge map post-processing (not filled), (f) removed non-closed polygons, (g) final edge map.

classification rate using a k-NN classifier.

The algorithm starts with an empty feature set and iteratively adds one feature at a time out of the candidate set, which complements the current feature subset best. We stop adding features if there is no feature found which raises the 6-classes classification performance any further (used as criterion value).

Classification: To obtain the criterion value for a potential feature set we carry out leave-one-out cross-validation (LOO-CV) runs with different choices for k used by the k-NN classifier. We allow only odd k-values between 1 and 9, which speeds up the subset selection (we also avoid draws during the voting in the 2-classes case). The k-value for the last added feature is used for the final classification. While we also tested the 2-classes result as criterion value, this almost always resulted in a considerably worse final classification performance (for 2-classes case as well as for 6-classes).

4 Experiments

4.1 Settings

The 627 images used throughout our experiments have been acquired between the years 2005 and 2009 at the Department of Gastroenterology and Hepatology (Medical University of Vienna) using a zoom-colonoscope (Olympus Evis Exera CF-Q160ZI/L, magnification factor set to 150). Lesions found during colonoscopy have been examined after application of dye-spraying with indigocarmine. Biopsies or mucosal resection have been performed in order to get a histopathological diagnosis. Biopsies have been taken from type 1, 2, and type 5 lesions. Type 3 and 4 lesions have been removed endoscopically. Out of all acquired images, histopathological classification resulted in the ground truth for our experiments shown in Table 2. Using LOO-CV, 626 out of 627 images are used as training set to classify the remaining image. This process is repeated for each image. While we are aware of the fact that subset selection with LOO-CV tends to overfitting, we are not able to split the image database into separate training and test sets due to the limited number of images (especially evident from class 3S).

Pit Type	**1**	**2**	**3S**	**3L**	**4**	**5**
2 classes	178		449			
6 classes	114	64	18	119	232	80

Table 2. Ground truth for our experiments.

4.2 Results

From Table 3 we see that the proposed method yields very encouraging results in the 2-classes and the 6-classes case – especially when combining different channels. The best result has been obtained by combining the red and the blue channel, resulting in an overall classification accuracy of about 97% for two classes and 88% for six classes. For all results presented, the subset selection ended up with a 1-NN classifier and the number of features finally used is rather low (D in Table 3) compared to a total number of 18, 36, and 54 available features for single channels, channel pairs and all channels, respectively.

We notice that in the 2-classes case the results for the non-neoplastic images are lower compared to the neoplastic images. This effect is especially apparent when using single channels. From Table 2 we see that the number of neoplastic images is about 1.6 times higher compared to the other class, which is one reason for this behavior. In the 6-classes case type 3S almost always delivers a poor classification rate, which most likely is due to the low number of images available for this class.

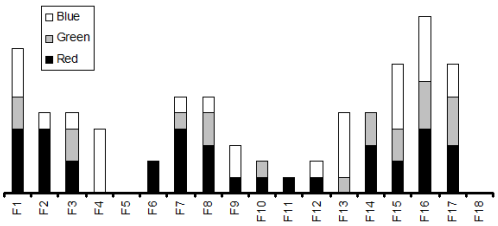

Figure 2. Selection statistics (by channel).

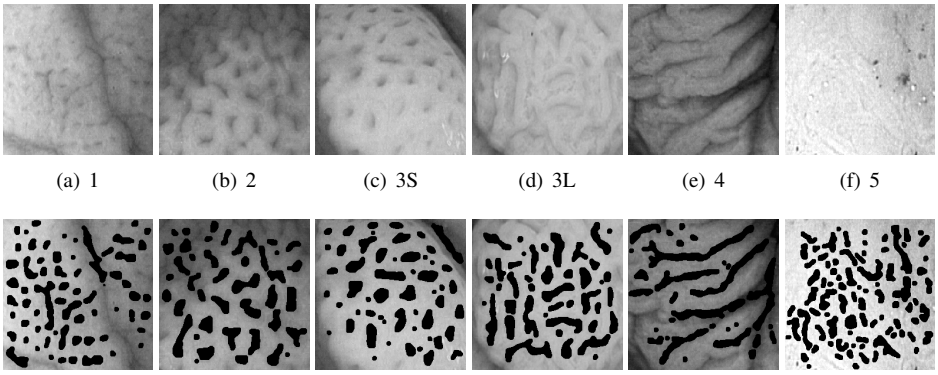

(a) 1 (b) 2 (c) 3S (d) 3L (e) 4 (f) 5

(g) 1 (h) 2 (i) 3S (j) 3L (k) 4 (l) 5

Figure 3. (a)-(f) Sample red channel for each pit type and (g)-(l) the pits detected.

	1	2	3S	3L	4	5	Total	*D*
R	76		95				**90**	11
	72	64	56	78	77	73	**74**	
G	78		91				**87**	8
	68	69	33	82	77	68	**73**	
B	75		92				**87**	6
	63	52	39	76	80	69	**71**	
RB	93		98				**97**	19
	91	88	61	91	88	84	**88**	
RG	84		96				**93**	14
	81	81	67	83	85	80	**83**	
GB	85		95				**92**	11
	76	80	56	83	88	69	**81**	
RGB	91		96				**94**	13
	83	83	56	87	90	83	**86**	

Table 3. Classification rates obtained by different color channel combinations along with the feature vector dimensions.

Fig. 2 shows how often a specific feature was chosen on average by the feature selection. Clearly dominating features are F1 and F15 to F17, which are all based on pixel intensities within the detected pit areas. The most frequently selected polygon-based features are F2, F4, and F9. These features are also used for the top result.

5 Conclusion and Future Research

We conclude that an automated pit pattern classification system based on edge features is feasible. This has been shown by the very promising results we already achieve. If we combine different color channels for the classification the results are improved even more.

However, the results presented in this work should be considered more as a demonstration of feasibility since we are aware of the fact that the subset selection tends to produce overfitted results. Hence, in future work we will compare our current approach to LOO-CV with a subset selection carried out for each image to be classified. We will also focus on analyzing the different features in more detail and improve them to be able to avoid using feature subset selection at all.

References

[1] M. J. Bruno. Magnification endoscopy, high resolution endoscopy, and chromoscopy; towards a better optical diagnosis. *Gut*, 52(4):7–11, 2003.

[2] J. Canny. A computational approach to edge detection. *IEEE Trans Pattern Anal Mach Intell*, 8(6):679–698, 1986.

[3] M. Häfner, A. Gangl, M. Liedlgruber, A. Uhl, A. Vécsei, and F. Wrba. Combining Gaussian Markov random fields with the discrete wavelet transform for endoscopic image classification. In *Proc of the 17th Int Conf on Digital Signal Processing (DSP'09)*, 2009.

[4] M. Häfner, R. Kwitt, A. Uhl, A. Gangl, F. Wrba, and A. Vécsei. Computer-assisted pit-pattern classification in different wavelet domains for supporting dignity assessment of colonic polyps. *Pattern Recognition*, 42(6):1180–1191, 2008.

[5] S. Kato, K. Fu, Y. Sano, T. Fujii, Y. Saito, T. Matsuda, I. Koba, S. Yoshida, and T. Fujimori. Magnifying colonoscopy as a non-biopsy technique for differential diagnosis of non-neoplastic and neoplastic lesions. *World J Gastroenterol*, 12(9):1416–1420, 2006.

[6] S. Kudo, S. Hirota, T. Nakajima, S. Hosobe, H. Kusaka, T. Kobayashi, M. Himori, and A. Yagyuu. Colorectal tumours and pit pattern. *J Clin Pathol*, 47:880–885, 1994.

[7] S. Kudo, S. Tamura, T. Nakajima, H. Yamano, H. Kusaka, and H. Watanabe. Diagnosis of colorectal tumorous lesions by magnifying endoscopy. *Gastrointest Endosc*, 44(1):8–14, 1996.

[8] M. S. Nixon and A. S. Aguado. *Feature Extraction & Image Processing*. Academic Press, 2nd edition, 2008.

[9] K. Zuiderveld. Contrast limited adaptive histogram equalization. In P. S. Heckbert, editor, *Graphics Gems IV*, pages 474–485. Morgan Kaufmann, 1994.